Discover Chemical Engineering

Research

Removal of acid red dye 1 from textile wastewater by heterogenous photocatalytic ozonation employing titanium dioxide and iron zeolite

Muhammad Raashid[1] · Mohsin Kazmi[1] · Amir Ikhlaq[2] · Muhammad Sulaiman[1] · Adeela Akram[1] · Aliha Afaf[1] · Sidra Shafaqat[1] · Zafar Masood[2] · Abdul Mannan Zafar[3] · Saleh Al-Farraj[4] · Mika Sillanpää[5,6,7,8,9,10,11,12]

Received: 24 May 2024 / Accepted: 18 July 2024
Published online: 01 August 2024

Abstract
Clean water is a necessity for all life to survive and flourish. However, natural waters are being continuously contaminated due to the release of waste streams in water. Hence, it is important to remove pollutants from wastewater to fulfill human needs. Conventional treatment methods are neither efficient nor economical for wastewaters that especially contain refractory toxic pollutants. This requires novel techniques like Advanced oxidation processes (AOPs), that may successfully degrade persistent micropollutants more efficiently. In this study, an azo dye Acid Red 1 was removed by three AOPs, namely Photocatalytic oxidation, Ozonation and Photocatalytic Ozonation, by employing heterogenous catalysts. TiO_2 was used as photocatalyst, whereas Fe-Zeolite has been further added as Ozonation catalyst. The study revealed that photocatalysis degraded only 28% Acid red dye after 15 min, whereas for ozonation, the degradation percentage was 95% in same time. In combined photocatalytic ozonation process using TiO_2, 95% degradation was achieved in just 9 min and treatment time further reduced to 5 min when Fe-zeolite was added. Optimization studies for initial concentration, UV intensity and catalyst loading were performed. Finally, rate constants and Electrical Energy per Order (EEO) values were determined for all AOPs, and mechanism was proposed.

Keywords Advanced oxidation processes · Wastewater treatment · Photocatalytic ozonation · Fe zeolite · Acid red dye

✉ Abdul Mannan Zafar, Abdul.Zafar@tii.ae; Muhammad Raashid, engr_raashid@uet.edu.pk; Mohsin Kazmi, drkazmi@uet.edu.pk; Amir Ikhlaq, aamirikhlaq@uet.edu.pk; Muhammad Sulaiman, m.sulaiman@uet.edu.pk; Adeela Akram, adeelaakrambajwa@gmail.com; Aliha Afaf, alihaafaf995@gmail.com; Sidra Shafaqat, sidashafaqat1044@gmail.com; Zafar Masood, engineerzafar71@gmail.com; Saleh Al-Farraj, alfarraj@ksu.edu.sa; Mika Sillanpää, mikaesillanpaa@gmail.com | [1]Department of Chemical, Polymer and Composite Materials Engineering, University of Engineering and Technology Lahore, Kala Shah Kaku Campus, Punjab 39021, Pakistan. [2]Institute of Environmental Engineering and Research, University of Engineering and Technology, GT Road, Lahore 54890, Punjab, Pakistan. [3]Biotechnology Research Center, Technology Innovation Institute, P.O. Box 9639, Masdar City, Abu Dhabi, United Arab Emirates. [4]Department of Zoology, College of Science, King Saud University, Riyadh, Saudi Arabia. [5]Functional Materials Group, Gulf University for Science and Technology, 32093 Mubarak Al-Abdullah, Kuwait. [6]School of Technology, Woxsen University, Hyderabad, Telangana, India. [7]Centre of Research Impact and Outcome, Chitkara University Institute of Engineering and Technology, Chitkara University, Rajpura 140401, Punjab, India. [8]Division of Research & Development, Lovely Professional University, Phagwara 144411, Punjab, India. [9]Adnan Kassar School of Business, Lebanese American University, Beirut, Lebanon. [10]Department of Chemical Engineering, School of Mining, Metallurgy and Chemical Engineering, University of Johannesburg, P. O. Box 17011, Doornfontein 2028, South Africa. [11]Department of Civil Engineering, University Centre for Research & Development, Chandigarh University, Gharuan, Mohali, Punjab, India. [12]Sustainability Cluster, School of Advanced Engineering, UPES, Bidholi, Dehradun 248007, Uttarakhand, India.

1 Introduction

Water is basic resource needed to sustain life and has no substitute, as living organisms are primarily composed of water. Water is needed not only water for humans, but also for survival of flora and fauna [1]. In addition, water is extensively utilized in irrigation, industries, urban centres, energy and manufacturing in such a high demand that lot of world population is suffering from water scarcity as recognized by the United Nation's SDG No. 6 namely Clean Water and Sanitation [2]. When a country is using 25% or more of its water resources, it is said to be facing water stress. At present, 40% of the world is facing water stress that includes reduced water availability per capita and deterioration of basic water quality parameters such as salinity and organics [3]. Rapid industrialization and population growth increased consumption of potable and freshwater which generates large volume of wastewater at alarming rate, especially in developing countries [4–6]. Approximately 80% of wastewater is discharged back untreated into receiving water bodies. Wastewater treatment is an important method to decontaminate polluted water sources [7].

The traditional techniques for wastewater treatment are classified as primary, secondary, and tertiary processes. These techniques include sedimentation, flotation, activated sludge process, membrane technologies, coagulation, filteration [8]. These traditional methods are unable to remove complex pollutants such as micropollutants, and thus novel treatment methods such as nanotechnology and catalytic processes are required [9]. Dyes have multiple applications in industries and seem difficult to degrade due to their complex molecular nature. However, due to their coloring ability, dyes are popular model pollutants in order to study a wastewater treatment process [10]. Textile wastewater can be carcinogenic in nature and is responsible for various adverse health effects [11]. More than ten thousand dyes have been commercially synthesized with industrial output of 0.8 million Metric Tons per year globally, and the unutilized waste dyes becomes textile wastewater [12]. The minimum and maximum water consumption by textile industry can be as low as 3 and reaches as high as 932 L per kilogram, respectively [13]. Textile industry is declared as large water volume consuming industries and almost 53% of industry is water inefficient [14].

Advanced Oxidation Processes (AOPs) have been evolved suitable option to address the issues related to textile industrial wastewater. AOP offers promising results for removal of complex and persistent organic pollutants that are otherwise not degraded in conventional wastewater methods [15, 16]. Some of the well-known AOPs include photocatalysis, ozonation which is usually catalytic, and the classic Fenton Processes [17]. In photocatalysis, usually a heterogenous photocatalyst is used that is activated with the use of a UV source photons. The advantages of photocatalysis include no additional chemicals, availability of inexpensive photocatalysts and affordable energy economics [18]. In catalytic ozonation, usually a homogenous catalyst that provides hydroxyl ions such as Hydrogen Peroxide H_2O_2 is used. Ozone is powerful oxidant, and it can also be combined with heterogenous catalysts or metal ions or adsorbents [19]. Whereas Fenton or electro-Fenton processes aim to increase the production of oxidation radical species with the help of additional chemicals such as H_2O_2 and iron salts [20]. To determine and compare the energy costs of different AOPs, a term namely electrical energy per order (EEO) is used to estimate the power requirement and energy inputs. EEO is the energy required in electric units that will degrade 90% of a given pollutant per cubic meter of polluted water. The AOP process is defined as feasible and acceptable only if the value of EEO is less than 100 [21].

Photocatalytic Ozonation is a combined AOP that mixes the beneficial effects of photocatalysis and ozonation. It is considered advantageous because of synergy between photocatalysis and ozonation, a single reactor and short residence times. Photocatalytic Ozonation results in better pollutants removal as compared to photolysis or ozonation alone. The pollutants which are unable to be degraded and removed by usual AOPs can be easily removed in no time by photocatalytic ozonation. In literature, synergies of 1.2–7.5 times have been observed for combining ozonation and photocatalysis [22]. Some instances of the dyes that have been successfully degraded by photocatalytic ozonation include Reactive Red Dye also known as RR 194 [23], Brilliant Red X-3B, also known as X3B [24] and Acid Blue 113 dye [25]. It has been observed that most of the works use only photocatalyst when combining the two processes, and the traditional photocatalyst is titanium dioxide (TiO_2) [26]. Many new photocatalysts are being discovered; in fact novel catalyst development is a hot area of research, but still TiO_2 remains the catalyst of choice due to low cost, easy availability, stability and non-toxicity [27]. The uses of TiO_2 include, but are not limited to photocatalysis, water splitting, food, microbial decontamination and CO_2 reduction [28].

Some recent studies have suggested enhancing the pollutants removal rate by adding ozonation catalyst in addition to photocatalyst with promising results [29, 30]. Although their role is not widely established yet, Iron (Fe) ions can act as ozonation catalyst as identified by bicarbonate quenching studies [31, 32]. In this study, Acid Red 1 Dye has been used

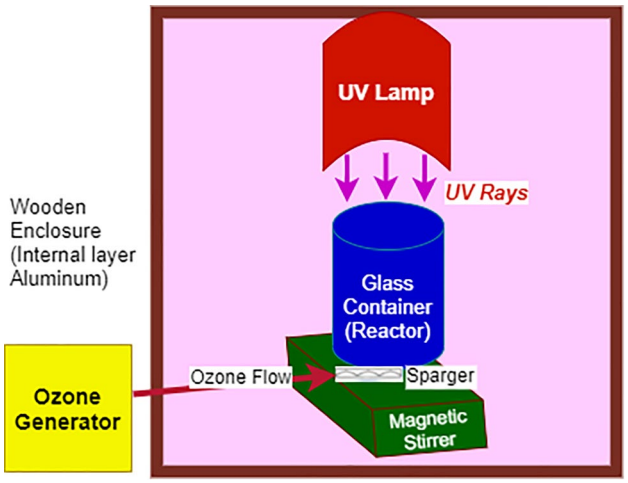

Fig. 1 Experimental setup for photocatalytic ozonation

Table 1 Properties of catalysts used

	Titanium dioxide	Zeolite
Particle size (μm)	0.5	0.40
Pore size (Å)	86	10
Surface area (m^2/g)	54	61.3

a model pollutant in order to study its removal by various AOPs to explore the synergy of photocatalysis and ozonation. In addition, the beneficial effect of adding Fe-zeolite has also been investigated.

2 Materials and methods

All reagents and materials including P25 form of TiO_2, Zeolite, Fe salts, Acid red 1 dye were purchased from local chemical market in analytical grades. For photoreactor, a glass beaker of 100 ml was used covered with a quartz glass plate to allow UV rays to pass. This container was placed right under a UV sourced lamp of make Quanzhiyan Electronic Co, country China, emitting UV-B of 310 nm. The reactor was positioned on a magnetic stirrer obtained from Quanbu, China. An inlet tube from ozone generator, of make Sterhen, was also provided connected to a sparger along with ozone traps on top of the setup. For the purpose of minimizing UV radiation loss, all the above-mentioned equipment was shielded and enclosed in a wooden rectangular box that has been internally coated on surface with aluminum foil. The schematic diagram of the proposed setup has been illustrated in Fig. 1.

The characterization of photocatalyst was carried out with the help of Scanning Electron Microscopy (SEM) imagery, particle size and point of zero charge. Some of the noteworthy properties of the catalysts were already specified by the vendor and were used as such, including particle size in μm, pore size in Å and specific surface area in m^2/g. These properties are specified in Table 1. Whereas the points of zero charge were determined experimentally, and the values were found out to be 6.6 ± 0.2 for titanium dioxide and 6.5 ± 0.2 for zeolite.

The effect of initial concentration on the degradation of dye was observed at four values for the Acid red 1 dye i.e., 100 mg/L to 400 mg/L with an interval of 100 mg/L. In addition, a combination of three different catalyst loadings with three different additions of Fe-Zeolite were used. Photocatalyst dose varied as 200 mg/L, 300 mg/L, and 400 g/L. The length of experiment for each run was set at 10 min, as this was sufficient time for complete degradation of dye (> 99%) in the combined process, as observed later. Fe-Zeolite was also added in three quantities, i.e., 10, 20 and 30%. The samples to determine residual concentration of dye were withdrawn at times 0, 1, 2, 3, 5, 7, and 10 min. To analyze the concentration of Acid red 1 dye, a UV–visible spectrophotometer was used. Prior to analysis, a standard curve was developed, by which the concentration of the dye could be determined. A linear standard curve resulted, in which the values of limit of detection and limit of quantitation were found out to be 0.016 and 0.049 mg/L, respectively, with the help of statistical regression analysis.

The UV lamp used for irradiation used wavelength of 310 nm, and therefore came under classification of UVB. Three lamp powers could be used for operation, i.e., 5, 10 and 15 W. The surface area of the reactor was fixed, so by varying the lamp power, the UV intensity changed and therefore the effect of UV intensity on degradation on dye could be determined. Electricity requirement for ozone generator was 15 W, and it produced 100 mg/hour of ozone flow rate. The rpm used for stirring was 2000 in the magnetic stirrer, because stirring above was liable to occasional spilling of reactor contents, which were set at neutral pH. All experiments were conducted on room temperature in an air-conditioned room, so that temperature remained fixed. The selected methodology has been summarized in Fig. 2.

3 Results and discussion

3.1 Characterization of catalysts

The SEM image of the photocatalyst has been produced in Fig. 3. SEM is an important analytical technique for material samples, that can characterize organic materials, metals, and polymers. An electron beam of 200–30,000 electron volts is used along with provision of vacuum to produce magnified images of up to 300,000 times [33].

The photocatalyst was also characterized by the experimentally determined BET surface area, and point of zero charge. Table 2 presents these experimentally detemined values as well as other important properties of both catalysts as supplied by the manufacturer, such as particle size in μm, pore size in Å, dry composition, and thermal stability temperature in °C.

The FTIR analysis of the zeolite before and after Fe-coating are given in Fig. 4. The major difference between both graphs can be noted at the peak of 1442 cm^{-1}, as per which the availability of aromatic compounds and presence of Fe that had been coated on zeolite can be confirmed.

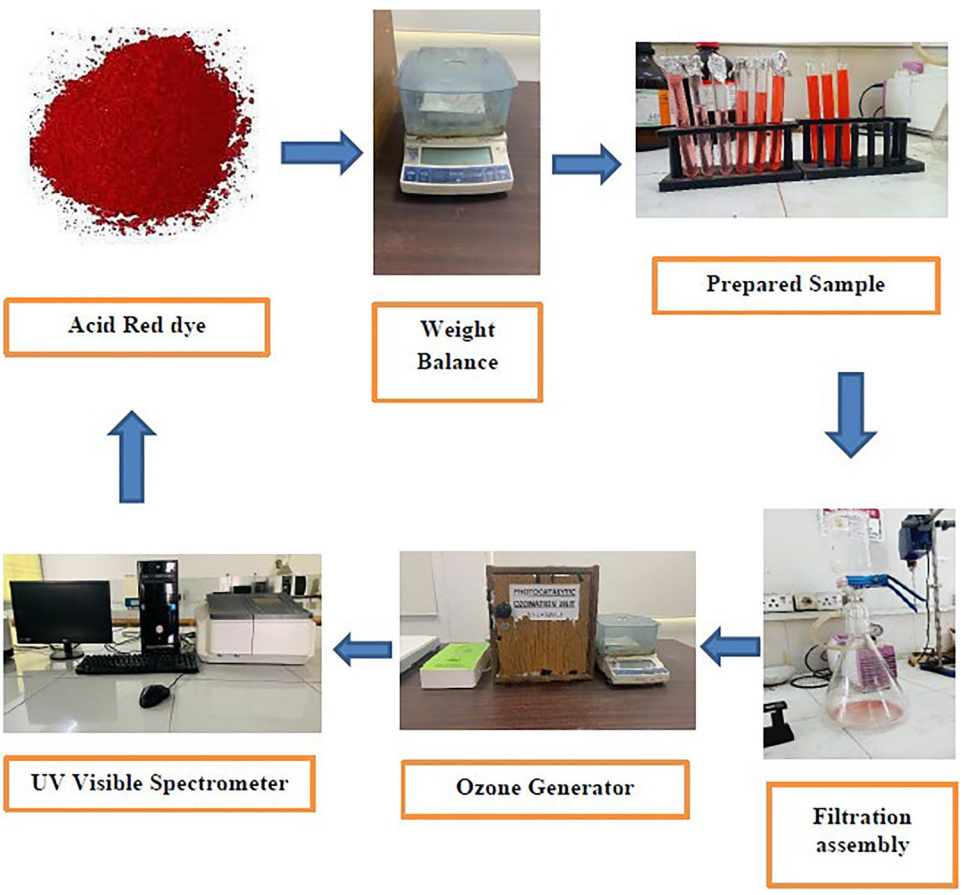

Fig. 2 Methodology for experimentation and analysis

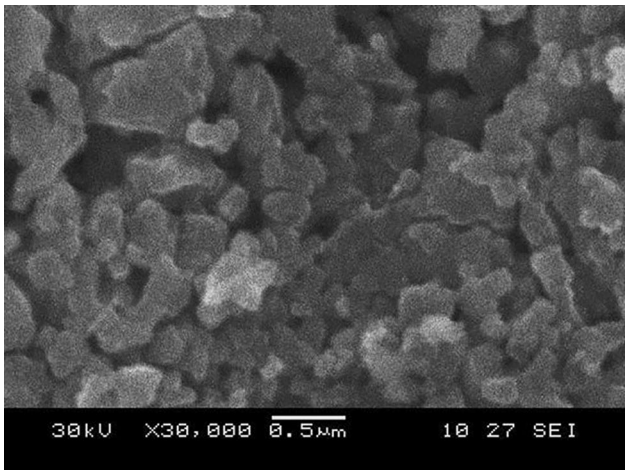

Fig. 3 SEM image of photocatalyst TiO_2

Table 2 Properties of catalysts used

	Titanium dioxide	Zeolite
Composition (Dry)	TiO_2	$2Na_2O$-Al_2O_3-1.75SiO_2-$6H_2O$
Thermal decomposition	400 °C (phasewise)	700 °C
Particle size (µm)	0.5	0.40
Pore size (Å)	86	10
BET Surface area (m^2/g)	54	61.3
Points of zero charge	6.5 ± 0.2	6.6 ± 0.2

3.2 Degradation studies

Figure 5 shows the degradation of Acid Red 1 Azo Dye by different Advanced Oxidation Processes over time range of 10 min. The Acid Red Dye is degraded by (i) Ozone only (ii) Photocatalysis only while using TiO_2 as photocatalyst (iii) Combined Photocatalytic Ozonation with TiO_2 as catalyst photocatalyst (iii) Photocatalytic Ozonation with TiO_2 and Fe-Zeolite as catalysts. All values obtained are for 100 mg/L initial concentration, 10 W UV lamp power, and catalyst loading of 0.3 g/L TiO_2 along with 20% Fe-Zeolite, as these are the most optimum values for the combined photocatalytic ozonation process, as determined later. When exposed to UV-B in presence of photocatalyst, the dye solution gradually decolourized owing to various radical changes and chemical decomposition procedure [34].

Since the reaction slows over time, it makes more sense to compare the degradation obtained at shorter time intervals. Therefore, the degradation values for all the above mentioned AOPs have been compared at 3 min in Fig. 6. Some degradation, i.e. 43% was observed with ozonation alone without using any catalyst, whereas UV alone with TiO_2 resulted in roughly 12% degradation at the same time. Once again, we can see, that the combined photocatalytic ozonation with combined catalysts namely TiO_2 and Fe-Zeolite is the fastest process, that achieved 91% degradation is 3 min. The increased degradation is owed to the synergy between photocatalysis in range of 254–354 nm for TiO_2 and ozonation below 320 nm where ozone degrades rapidly into reactive species, while preventing electron–hole pairs to recombine [35, 36]. Similar successful results for degradation of dyes by photocatalytic ozonation have been reported by other scientists [34, 37, 38].

3.3 Effect of initial concentration

Initial concentration is an important parameter that affects the removal rate of pollutants in photocatalytic ozonation [39]. The effect of initial concentration on the removal of Acid Red Dye 1 is presented in Fig. 7.

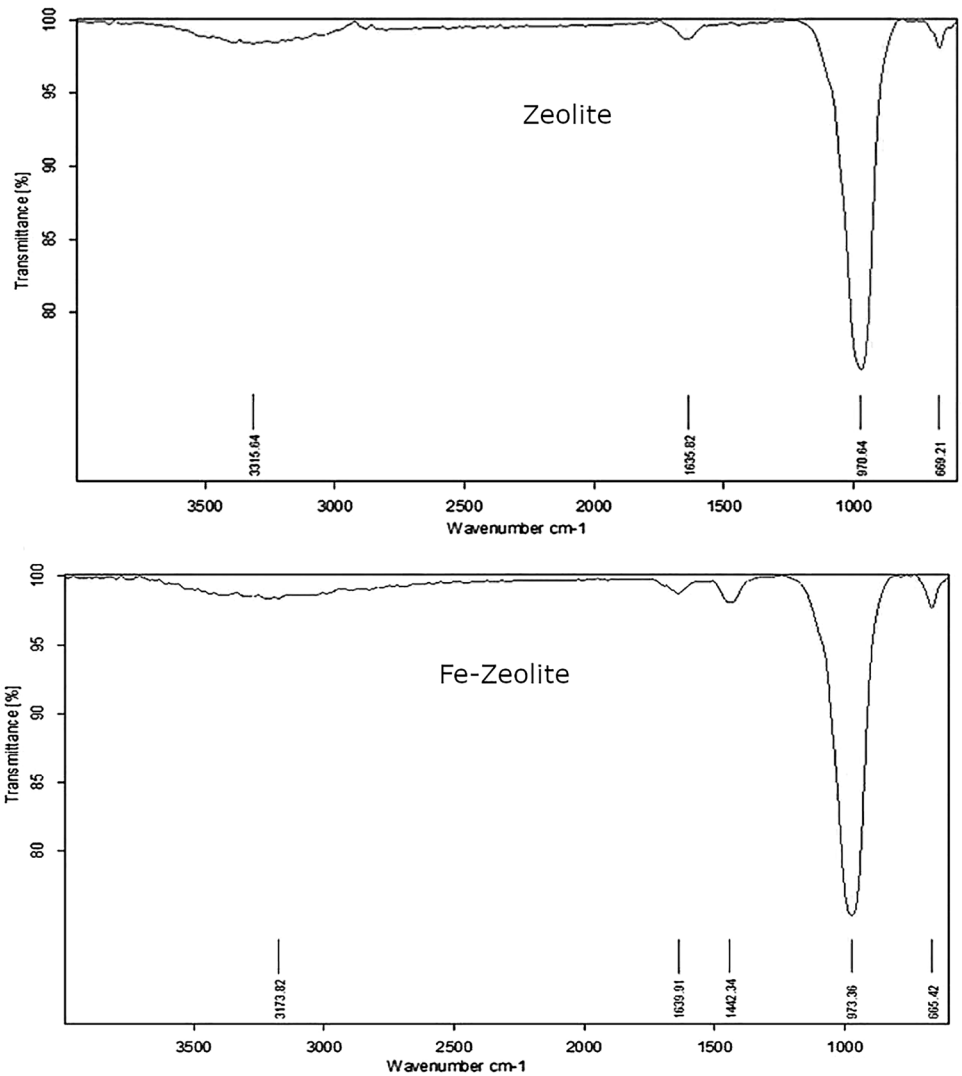

Fig. 4 FTIR of zeolite (Before and after Fe-coating)

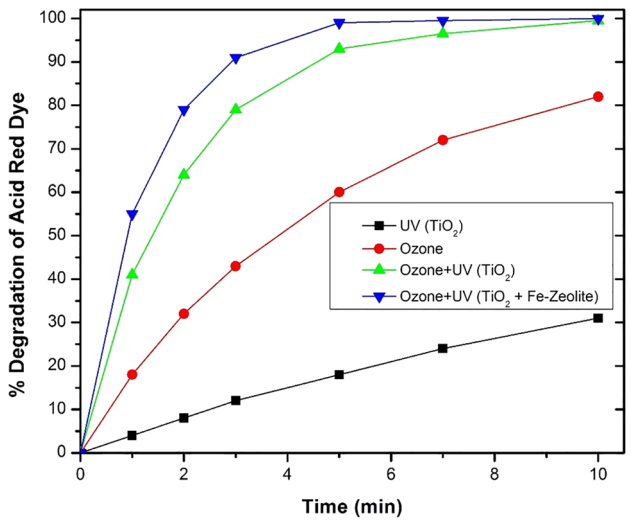

Fig. 5 Degradation of acid red 1 dye by various AOPs over time

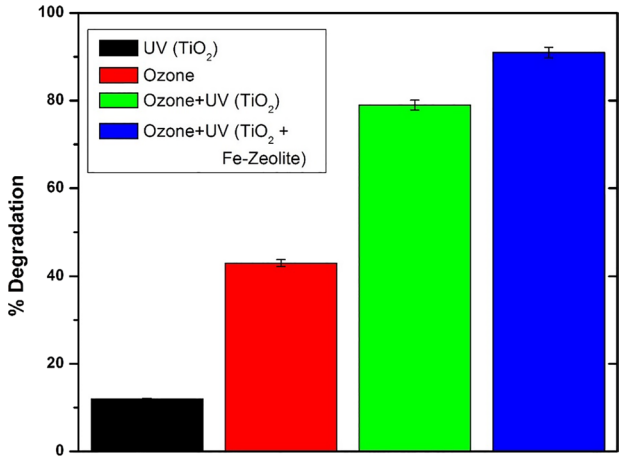

Fig. 6 Degradation of acid red 1 dye by various AOPs at 3 min

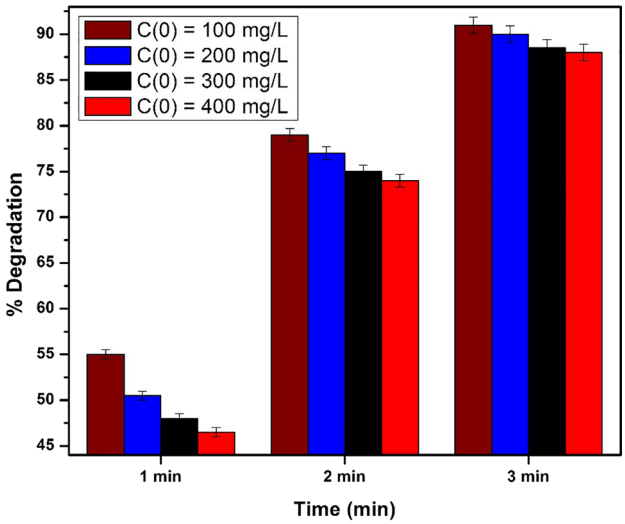

Fig. 7 Effect of initial concentration on degradation of acid red dye till 3 min

The values of initial concentration are varied between 100 and 400 mg/L with increment of 100 mg/L. As already discussed, the reaction slows over time, therefore it makes more sense to make comparisons at shorter time intervals. So, the time intervals selected for comparison are 1, 2, and 3 min. All comparisons have been made at 10 W UV lamp power, and catalyst loading of 0.3 g/L TiO_2 along with 20% Fe-Zeolite. As evident from Fig. 7, an increase in initial concentration has resulted in a notable decrease in the degradation or removal percentages. This can be owed to the fact that same reactor space, same UV intensity, same amount of ozone and same catalyst sites are now faced with increased task of removing more pollutants. The increased saturation of catalyst active sites results in reduction of removal with increasing the initial concentration. Similar effects have been observed for Amido Black [40] and Methylene Blue for photocatalytic ozonation and other AOPs.

3.4 Variation of UV intensity

Three different lamp electric powers i.e., 5, 10 and 15 W were used for degradation of the pollutant. The lamp powers of 5, 10 and 15 W correspond to UV intensities of 65, 130 and 195 W/m^2, respectively. All values are resulted from 100 mg/L initial concentration, and catalyst loading of 0.3 g/L TiO_2 along with 20% Fe-Zeolite. For the reasons already explained, the comparisons are made at short time intervals (Fig. 8). It can be observed in Fig. 8 that increasing the UV lamp power from 5 to 10 W results in increased degradation, however when lamp power is increased to 15 W, the degradation almost remains same. This may be explained by the reason that initially more UV means more degradation, because many catalyst sites are not being utilized and are still available. The increased degradation of pollutant with increased UV intensity is also reported elsewhere [41]. However, after a certain UV intensity, all catalyst sites are already being

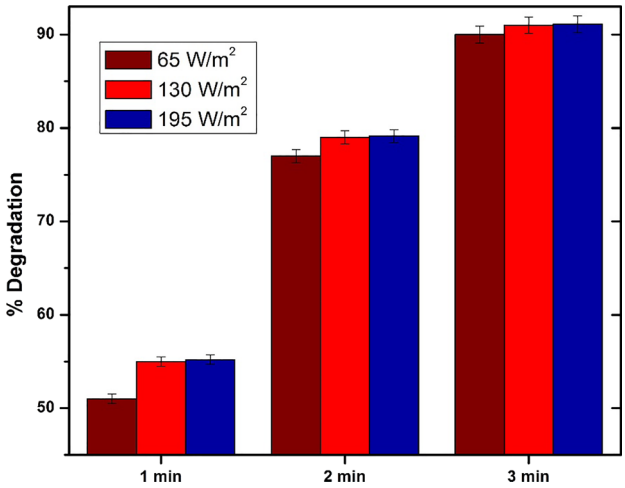

Fig. 8 Effect of UV intensity on degradation of acid red 1 dye at 1, 2 and 3 min

utilized. An additional increase in UV lamp power will bring no benefit and only an increase in energy costs, which are already significant for AOPs [42].

3.5 Effect of varying catalyst dose

Catalyst loading is the third operational parameter which effect on the degradation of the model pollutant Acid Red 1 Dye has been noted. In the combined processes, there are two catalysts namely TiO_2 and Fe-Zeolite, hence both their quantities have been varied. The degradation values in Fig. 9 are for 100 mg/L initial concentration and 10 W UV lamp power at a selected shorter time interval. Although it would have been desirable to use time-based plots on a single graph, the resulting figure is distorted and contains intermingling of lines, so the effect is not clearly observed. It can be deduced for Fig. 9 that a middle optimum value exists for catalyst loading. As the catalyst dose is increased, an increase in degradation percentage is observed. But further increasing the catalyst dose results in reduction of degradation percentage. This can be attributed to scattering and blockage of UV light and negatively affecting transport processes, in other words less irradiation reaching the pollutant [43]. The best value of catalyst quantities is observed as 0.3 g/L TiO_2 and 20% Fe-Zeolite. Similar trends have been observed for Acid Blue 113 azo dye [25].

3.6 Catalyst reuse

For investigating catalyst reuse properties, both the TiO_2 and Fe-Zeolite Catalysts were washed, heated and dried, and thereafter used in subsequent test runs. The initial concentration was taken as 100 mg/L whereas the percentage of

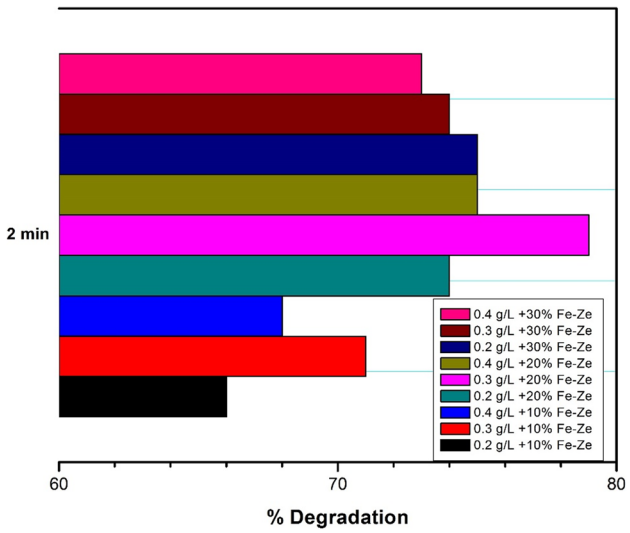

Fig. 9 Effect of catalyst dose and Fe-Zeolite loading on degradation of acid red 1 dye after 2 min

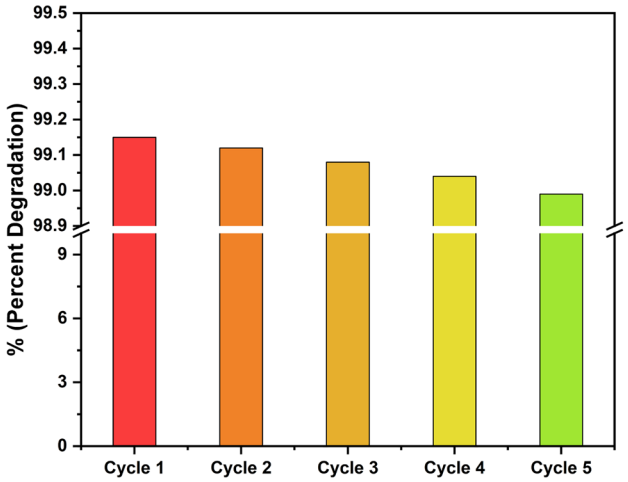

Fig. 10 Catalyst reuse performance measured by degradation percent of pollutant dye for 5 cycles

degradation was calculated after 6 min for each cycle while utilizing 130 W/m^2 UVC. Even after five cycles, the catalyst performance remains excellent as seen in Fig. 10.

3.7 Kinetics and mechanism

The kinetics of all the AOPs namely (i) Ozonation (ii) Photocatalysis with TiO_2 (iii) Combined Photocatalytic Ozonation with TiO_2 only (iv) Combined Photocatalytic Ozonation with TiO_2 and Fe-Zeolite have been plotted in Fig. 10 with acceptable values of R^2. For the purpose of finding values of rates, curve fitting technique has been applied while using Equation of type (1) in Fig. 11.

$$\frac{C}{C_0} = e^{-\frac{t}{\tau}} \tag{1}$$

where t is the time and τ is the retention time, the units for both these are in minutes.

The nature of curves in Fig. 11, i.e., exponential, and sequential curve fitting of exponential lines with reasonable values of R^2 indicate that all AOPs studied, i.e., ozonation, photocatalysis, and photocatalytic ozonation are following kinetics of pseudo-first-order kinetics. However, since all the curves have different slopes and shapes, the rates of reactions and rate constants are understandably varied. The pseudo-first order kinetics for above-mentioned AOPs is also widely reported in literature [44, 45]. The concentration of the Acid Red Dye 1 vs time has been plotted for all AOPs. It can be observed from Fig. 11 that all AOPs are able

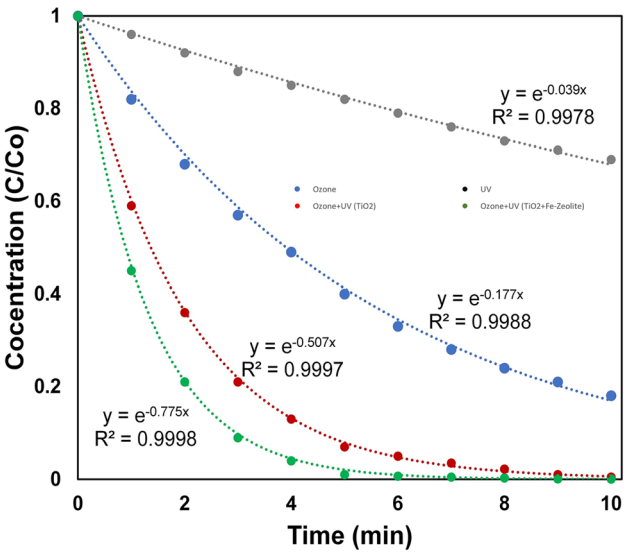

Fig. 11 Determination of rate constants for various AOPs for degradation of acid red 1 dye

to degrade the azo dye over time. Slowest process is observed for Photocatalysis with TiO_2 with a rate constant of 0.039 min^{-1}. While ozonation is comparatively a faster process with a rate constant of 0.177 min^{-1}. Even better is the combined process of photocatalytic ozonation, in which a rate constant of 0.507 min^{-1} has been observed. This shows a synergy of 2.35 times, as compared with the individual processes. If Fe-zeolite is added as well, the rate constant is improved by 1.53 times, and the synergy now climbs to 3.59 times. This suggest that the combined photocatalytic ozonation with both TiO_2 and Fe-Zeolite is the fastest process for degradation of Acid Red 1 Dye as corroborating with other works for other pollutants [46].

Although it is only frequently proposed, the exact mechanism of the combined process photocatalytic ozonation is still not totally clear. According to a review of the literature, there are various pathways by which photocatalytic ozonation destroys the reactant molecule. A synergistic behaviour in photocatalytic ozonation is caused by three reasons. I- Initially, as shown by Eqs. (2)–(5), ozone on the surface of TiO_2 produces $OH^{\cdot}$ radicals utilizing a series of steps in which an ozonide radical has acted as an intermediate. Ozone is substantially more beneficial than oxygen since it is a stronger oxidant and a better scavenger [24].

$$TiO_2 + hv \rightarrow e^- + h^+ \tag{2}$$

$$O_3 + e^- \rightarrow O_3^{\cdot -}(\text{Ozonide radical}) \tag{3}$$

$$O_3^{\cdot -} + H^+ \rightarrow HO_3^{\cdot -} \tag{4}$$

$$HO_3^{\cdot -} \rightarrow O_2 + OH^{\cdot} \tag{5}$$

(II) Second, ozone photolysis also contributes to the production of $OH^{\cdot}$ radicals. More $OH^{\cdot}$ radicals can then be created by the reaction of ozone with superoxide ion radicals. Equations (6)–(8) represent these steps [47–49].

$$O_3 + \left(H_2O, hv\right) \rightarrow H_2O_2 \tag{6}$$

$$H_2O_2 \rightarrow HO_2^-(\text{Ozonide radical}). \tag{7}$$

$$O_3 + HO_2^- \rightarrow HO_2^{\cdot} + O_3^{\cdot -} \rightarrow \cdots \rightarrow OH^{\cdot} \tag{8}$$

(III) Last but not the least, ozone effectively traps the photogenerated electrons, lowering the rate at which electrons recombine with holes. Superoxide radicals are produced because of oxygen trapping the photogenerated electrons. Ozone and these superoxide radicals may then interact further. Equations (9) and (10) illustrate these incidents [50].

$$e^- + O_2 \rightarrow O_2^{\cdot -} \tag{9}$$

$$O_2^{\cdot -} + O_3 \rightarrow O_3^{\cdot -} + O_2 \tag{10}$$

Moreover, the additional doping of iron ions enhances electron trapping, which prevents electron–hole recombination in the presence of UV radiation, see Equations (11)–(14). This is due to Fe^{3+} ions serving as possible electron- and hole-trapping sites, whereby suppressing the recombination of the charged particles generated by UV radiation. This increases their lifespans and improves their performance in general [51].

$$Fe^{3+} + e^- \rightarrow Fe^{2+} \tag{11}$$

$$Fe^{2+} + O_2 \rightarrow Fe^{3+} + O_2^{\cdot -} \tag{12}$$

$$Fe^{3+} + h^+ \rightarrow Fe^{4+} \tag{13}$$

$$Fe^{4+} + OH^- \rightarrow Fe^{3+} + OH \tag{14}$$

Table 3 Electrical energy per order (EEO) and rate constants for pseudo-first order kinetics for various AOPs

Process	P_{el} (kW)	Rate constants (min^{-1})	EEO (kWh m^{-3} $order^{-1}$)
O_3	0.015	0.177	32.54
$UV + TiO_2$	0.010	0.039	98.46
$O_3 + UV + TiO_2$ (TiO_2 only)	0.025	0.507	18.94
$O_3 + UV + TiO_2$ + Fe-Zeolite	0.025	0.775	12.38

The ozonide radicals $O_3^{\cdot -}$, HO_2^-, and $O_2^{\cdot -}$ are some of the oxygen species that have been identified as being present when ozonation is occuring, as evident from above equations. Moreover, the hydroxyl free radicals $OH^{\cdot}$ and $HO_3^{\cdot -}$ are produced when hydrogen and oxygen are combined. Likewise, $O_3^{\cdot -}$, $OH^{\cdot}$ and $HO_3^{\cdot}$ have been found as reactive species in photocatalysis, as per above equations. Nitric and organic peroxides can also be occasionally produced by photocatalysis [52]. The same oxygen reactive species as those stated above are reportedly present during ozonation, with $O_2^{\cdot -}$ and $OH^{\cdot}$ being more common [53].

3.8 Energy Considerations

After the discussion on kinetics and mechanism, finally we focus on determination of values of Electrical Energy per Order (EEO) using Eq. (15), as per the pseudo first-order kinetics already established for the dye in question. The EEO equation is applied one by one for all AOPs [54, 55].

$$EEO = \frac{38.4 \times P_{el}}{V \times k_{app}} \tag{15}$$

where P_{el} is electric power having units of kilowatts kW, V means volume of the reactor in liters L, and k_{app} is the pseudo-first-order rate constant with units of min^{-1}.

The values of EEO for various AOPs have been compared in Table 3. Here it can be seen that all the four AOPs produce EEO of less than 100. The combined process with both catalysts produces the lowest EEO figure of 12.38 kWh m^{-3} $order^{-1}$, indicating that is the most energy efficient AOP.

For comparison, values of EEO for other dyes as observed in literature are 29.43 kWh m^{-3} $order^{-1}$ for Basic Red 46 dye and 1.1976 kWh m^{-3} $order^{-1}$ Reactive Red [11, 56]. Therefore, the value of EEO is well within the range found in literature for degradation of dyes.

4 Conclusions

There is an urgent need to address the problem of water shortage, as evident from recognition by the United Nations in form of SDG No. 6 namely "Clean Water and Sanitation". Wastewater treatment is one of the best currently available options to overcome two simultaneous problems of water shortage and water contamination. AOPs are novel techniques that have been recently advocated to remove modern persistent micropollutants from water, of which Photocatalytic Ozonation holds considerate advantages. In this study, an Acid Red 1 dye based simulated textile wastewater was subject to various AOPs namely ozonation, photocatalysis, Photocatalytic ozonation with TiO_2 and lastly Photocatalytic Ozonation with TiO_2 and Fe-Zeolite. The combined process was able to degrade 99% pollutant in just 9 min, whereas adding Fe-Zeolite further reduces this time to 5 min. The optimized values of operational variables are 100 mg/L of initial concentration, UV lamp power of 10 W, and catalyst loading of 0.3 g/L TiO_2 along with 20% Fe-Zeolite. The combined photocatalytic ozonation with both catalysts reports rate constant of 0.775 min^{-1}, synergy of 3.59 times, and EEO of 12.38 kWh m^{-3} $order^{-1}$. Therefore, it is concluded that photocatalytic ozonation is very viable option for removal of micropollutants, such as dyes from contaminated aqueous solutions. But these promising AOPs are still plagued by issues of high energy requirements and exorbitant operating costs.

Additionally, there is a need to convert the existing laboratory or pilot plant setups to full fledge industrial wastewater treatment plants, or at least incorporation in existing industrial setups. Therefore, economics and upscaling of AOPs provide excellent opportunities for future works. As AOPs have excellent potential to simultaneously mitigate two major global problems, i.e., water pollution and water scarcity.

Author contributions Muhammad Raashid: Conceptualization, Methodology, Investigation, Resources, Supervision, Writing—Review and Editing; Mohsin Kazmi: Conceptualization, Resources, Writing—Review and Editing; Amir Ikhlaq: Conceptualization, Supervision, Writing—Review and Editing; Muhammad Sulaiman: Investigation, Resources; Adeela Akram: Investigation, Resources, Writing—Original Draft Preparation; Aliha Afaf: Investigation, Resources, Writing—Original Draft Preparation; Sidra Shafaqat: Investigation, Resources, Writing—Original Draft Preparation; Zafar Masood: Conceptualization, Methodology, Investigation, Resources, Writing—Review and Editing; Abdul Mannan Zafar: Investigation, Resources, Writing—Review and Editing; Saleh Al-Farraj: Writing—Review and Editing; Mika Sillanpää: Writing—Review and Editing.

Funding This research was funded by "University of Engineering and Technology Lahore". This project was supported by Researchers Supporting Project Number (RSP-2024R7) King Saud University, Riyadh, Saudi Arabia.

Data availability Data will be available on demand.

Declarations

Ethics approval The authors agreed that this original work has not been considered or submitted to any other journal during the submission to Environmental Science and Pollution Research. This work is not a part of any other article, it is solely submitted to this journal only. The results are not published elsewhere and previous work is cited considerably where authors found necessary.

Consent to participate All authors agreed to participate in this research and jointly prepared this manuscript considering ethical practices. No human/animal subject was examined or provided nanoparticles/drug delivery while conducting this research.

Consent for publish All authors agreed to publish this article in Environmental Science and Pollution Research.

Competing interests The authors declare no competing interests.

References

1. Ruidas D, Pal SC, Saha A, Chowdhuri I, Shit M. Hydrogeochemical characterization based water resources vulnerability assessment in India's first Ramsar site of Chilka lake. Mar Pollut Bull. 2022;184:114107. https://doi.org/10.1016/j.marpolbul.2022.114107.
2. Phuong NM, Chu NC, Van Thuan D, Ha MN, Hanh NT, Viet HDT, Minh Thu NT, Van Quan P, Thanh Truc NT. Novel removal of diazinon pesticide by adsorption and photocatalytic degradation of visible light-driven Fe-TiO_2/Bent-Fe photocatalyst. J Chem. 2019;2019:2678927. https://doi.org/10.1155/2019/2678927.
3. van Vliet MTH, Jones ER, Flörke M, Franssen WHP, Hanasaki N, Wada Y, Yearsley JR. Global water scarcity including surface water quality and expansions of clean water technologies. Environ Res Lett. 2021;16:24020.
4. Zafar AM, Javed MA, Hassan AA, Sahle-Demessie E, Harmon S. Biodesalination using halophytic cyanobacterium phormidium keutzingianum from brackish to the hypersaline water. Chemosphere. 2022;307:136082. https://doi.org/10.1016/j.chemosphere.2022.136082.
5. Zafar AM, Javed MA, Hassan AA, Mohamed MM. Groundwater remediation using zero-valent iron nanoparticles (nZVI). Groundw Sustain Dev. 2021;15:100694. https://doi.org/10.1016/j.gsd.2021.100694.
6. Zafar AM, Al Mosteka H, Aly Hassan A. Performance of immobilized microalgal strains for biodesalination of real seawater. Desalination. 2023;561:116704. https://doi.org/10.1016/j.desal.2023.116704.
7. Khan SAR, Ponce P, Yu Z, Golpîra H, Mathew M. Environmental technology and wastewater treatment: strategies to achieve environmental sustainability. Chemosphere. 2022;286:131532. https://doi.org/10.1016/j.chemosphere.2021.131532.
8. Raouf MEA, Maysour NE, Farag RK, Abdul-Raheim AM. Wastewater treatment methodologies, review article. Int J Environ Agri Sci. 2019;3:18.
9. Kesari KK, Soni R, Jamal QMS, Tripathi P, Lal JA, Jha NK, Siddiqui MH, Kumar P, Tripathi V, Ruokolainen J. Wastewater treatment and reuse: a review of its applications and health implications. Water Air Soil Pollut. 2021;232:208. https://doi.org/10.1007/s11270-021-05154-8.
10. Kamran U, Bhatti HN, Noreen S, Tahir MA, Park S-J. Chemically modified sugarcane bagasse-based biocomposites for efficient removal of acid red 1 dye: kinetics, isotherms, thermodynamics, and desorption studies. Chemosphere. 2022;291:132796. https://doi.org/10.1016/j.chemosphere.2021.132796.

11. Zafar AM, Naeem A, Minhas MA, Hasan MJ, Rafique S, Ikhlaq A. Removal of reactive dyes from textile industrial effluent using electrocoagulation in different parametric conditions of aluminum electrodes. Total Environ Adv. 2024;9:200087. https://doi.org/10.1016/j.teadva.2023.200087.
12. Wang X, Jiang J, Gao W. Reviewing textile wastewater produced by industries: characteristics, environmental impacts, and treatment strategies. Water Sci Technol. 2022;85:2076–96. https://doi.org/10.2166/wst.2022.088.
13. Raashid M, Kazmi M, Ikhlaq A, Iqbal T, Sulaiman M, Zafar AM, Aly Hassan A. Degradation of sulfoxaflor pesticide in aqueous solutions utilizing photocatalytic ozonation with the simultaneous use of titanium dioxide and iron zeolite catalysts. Water. 2023;15:1283. https://doi.org/10.3390/w15071283.
14. Naqvi SA, Arshad M, Farooq A, Nadeem F. Implementation of sustainable practices in textile processing mills of Lahore, Pakistan. Pol J Environ Stud. 2020;29:1–9. https://doi.org/10.1524/pjoes/99062.
15. Giannakis S, Lin K-YA, Ghanbari F. A review of the recent advances on the treatment of industrial wastewaters by sulfate radical-based advanced oxidation processes (SR-AOPs). Chem Eng J. 2021;406:127083.
16. Priyadarshini M, Das I, Ghangrekar MM, Blaney L. Advanced oxidation processes: performance, advantages, and scale-up of emerging technologies. J Environ Manage. 2022;316:115295. https://doi.org/10.1016/j.jenvman.2022.115295.
17. Deng Y, Zhao R. Advanced oxidation processes (AOPs) in wastewater treatment. Curr Pollut Rep. 2015;1:167–76.
18. Loeb SK, Alvarez PJJ, Brame JA, Cates EL, Choi W, Crittenden J, Dionysiou DD, Li Q, Li-Puma G, Quan X, Sedlak DL, David Waite T, Westerhoff P, Kim J-H. The technology horizon for photocatalytic water treatment: sunrise or sunset? Environ Sci Technol. 2019;53:2937–47. https://doi.org/10.1021/acs.est.8b05041.
19. Hu Q, Zhang M, Xu L, Wang S, Yang T, Wu M, Lu W, Li Y, Yu D. Unraveling timescale-dependent Fe-MOFs crystal evolution for catalytic ozonation reactivity modulation. J Hazard Mater. 2022;431:128575. https://doi.org/10.1016/j.jhazmat.2022.128575.
20. Guo D, Liu Y, Ji H, Wang C-C, Chen B, Shen C, Li F, Wang Y, Lu P, Liu W. Silicate-enhanced heterogeneous flow-through electro-fenton system using iron oxides under nanoconfinement. Environ Sci Technol. 2021;55:4045–53. https://doi.org/10.1021/acs.est.1c00349.
21. Lee C-G, Javed H, Zhang D, Kim J-H, Westerhoff P, Li Q, Alvarez PJJ. Porous electrospun fibers embedding TiO2 for adsorption and photocatalytic degradation of water pollutants. Environ Sci Technol. 2018;52:4285–93. https://doi.org/10.1021/acs.est.7b06508.
22. Mehrjouei M, Müller S, Möller D. A review on photocatalytic ozonation used for the treatment of water and wastewater. Chem Eng J. 2015;263:209–19.
23. Yildirim AÖ, Gül S, Eren O, Kucsvuran E. A comparative study of ozonation, homogeneous catalytic ozonation, and photocatalytic ozonation for CI reactive Red 194 azo dye degradation, CLEAN–soil, air. Water. 2011;39:795–805.
24. Sun J, Yan X, Lv K, Sun S, Deng K, Du D. Photocatalytic degradation pathway for azo dye in TiO2/UV/O3 system: hydroxyl radical versus hole. J Mol Catal A Chem. 2013;367:31–7. https://doi.org/10.1016/j.molcata.2012.10.020.
25. Bagheri F, Chaibakhsh N. Efficient visible-light photocatalytic ozonation for dye degradation using Fe2O3/MoS2 nanocomposite. Sep Sci Technol. 2021;56:3022–32. https://doi.org/10.1080/01496395.2020.1861018.
26. Mecha AC, Chollom MN. Photocatalytic ozonation of wastewater: a review. Environ Chem Lett. 2020;18:1491–507.
27. Gopinath KP, Madhav NV, Krishnan A, Malolan R, Rangarajan G. Present applications of titanium dioxide for the photocatalytic removal of pollutants from water: a review. J Environ Manage. 2020;270:110906. https://doi.org/10.1016/j.jenvman.2020.110906.
28. Arun J, Nachiappan S, Rangarajan G, Alagappan RP, Gopinath KP, Lichtfouse E. Synthesis and application of titanium dioxide photocatalysis for energy, decontamination and viral disinfection: a review. Environ Chem Lett. 2023;21:339–62. https://doi.org/10.1007/s10311-022-01503-z.
29. Raashid M, Kazmi M, Ikhlaq A, Iqbal T, Sulaiman M, Shakeel A. Degradation of aqueous CONFIDOR®Pesticide by simultaneous TiO2 photocatalysis and Fe-Zeolite catalytic ozonation. Water. 2021;13:3327.
30. Raashid M, Kazmi M, Ikhlaq A, Iqbal T, Sulaiman M, Zafar AM, Aly Hassan A. Degradation of sulfoxaflor pesticide in aqueous solutions utilizing photocatalytic ozonation with the simultaneous use of titanium dioxide and iron zeolite catalysts. Water. 2023. https://doi.org/10.3390/w15071283.
31. Amir Ikhlaq M, Raashid A, Akram M, Kazmi SF. Removal of methylene blue dye from aqueous solutions by adsorption in combination with ozonation on iron loaded sodium zeolite: role of adsorption. Desalination Water Treat. 2021. https://doi.org/10.5004/dwt.2021.27744.
32. Ikhlaq A, Javed F, Munir MS, Hussain S, Joya KS, Zafar AM, Khurram Saleem Joya. Application of heterogeneous iron loaded zeolite A catalyst in photo-Fenton process for the removal of safranin in wastewater. DWT. 2019;148:152–61. https://doi.org/10.5004/dwt.2019.23903.
33. A. Mohammed, A. Abdullah, Scanning electron microscopy (SEM): A review, in: Proceedings of the 2018 International Conference on Hydraulics and Pneumatics—HERVEX, Băile Govora, Romania, 2018: pp. 7–9.
34. Joseph CG, Puma GL, Bono A, Krishnaiah D. Sonophotocatalysis in advanced oxidation process: a short review. Ultrason Sonochem. 2009;16:583–9.
35. Fathinia M, Khataee A, Vahid B, Joo SW. Scrutinizing the vital role of various ultraviolet irradiations on the comparative photocatalytic ozonation of albendazole and metronidazole: integration and synergistic reactions mechanism. J Environ Manage. 2020;272:111044. https://doi.org/10.1016/j.jenvman.2020.111044.
36. Shukla S, Pandey H, Singh P, Tiwari AK, Baranwal V, Pandey AC. Synergistic impact of photocatalyst and dopants on pharmaceutical-polluted waste water treatment: a review. Environ Pollut Bioavailability. 2021;33:347–64.
37. Sheydaei M, Soleimani D, Ayoubi-Feiz B. Simultaneous immobilization of Dy2O3, graphite and TiO2 to prepare stable nanocomposite for visible light assisted photocatalytic ozonation of a wastewater: modeling via artificial neural network. Environ Technol Innov. 2020;17:100512. https://doi.org/10.1016/j.eti.2019.100512.
38. Hosseini SMP, Chaibakhsh N. Efficient dye removal using Fe3O4.MnO2.MoS2 nanocomposite in optimized photocatalytic ozonation process. Ozone Sci Eng. 2022. https://doi.org/10.1080/01919512.2022.2109590.
39. Zhang L, Meng G, Liu B, Ge X. Heterogeneous photocatalytic ozonation of sulfamethoxazole by Z-scheme Bi2WO6/TiO2 heterojunction: performance, mechanism and degradation pathway. J Mol Liq. 2022;360:119427. https://doi.org/10.1016/j.molliq.2022.119427.
40. Hamdi D, Mansouri L, Park Y, Srivastava V, Sillanpaa M, Bousselmi L. Development of a continuous photo-catalytic/ozonation system: application on amido black removal from water. Ozone Sci Eng. 2022;44:545–65. https://doi.org/10.1080/01919512.2021.2004877.

41. Rafiq A, Ikram M, Ali S, Niaz F, Khan M, Khan Q, Maqbool M. Photocatalytic degradation of dyes using semiconductor photocatalysts to clean industrial water pollution. J Ind Eng Chem. 2021;97:111–28. https://doi.org/10.1016/j.jiec.2021.02.017.
42. Lincho J, Zaleska-Medynska A, Martins RC, Gomes J. Nanostructured photocatalysts for the abatement of contaminants by photocatalysis and photocatalytic ozonation: an overview. Sci Total Environ. 2022;837:155776. https://doi.org/10.1016/j.scitotenv.2022.155776.
43. Norabadi E, Panahi AH, Ghanbari R, Meshkinian A, Kamani H, Ashrafi SD. Optimizing the parameters of amoxicillin removal in a photocatalysis/ozonation process using Box-Behnken response surface methodology. Desalin Water Treat. 2020;192:234–40.
44. Malakootian M, Mahdizadeh H, Dehdarirad A, Amiri Gharghani M. Photocatalytic ozonation degradation of ciprofloxacin using ZnO nanoparticles immobilized on the surface of stones. J Dispers Sci Technol. 2019;40:846–54. https://doi.org/10.1080/01932691.2018.1485580.
45. Ikhlaq A, Naeem A, Rizvi OS, Akram A, Zafar AM, Qi F, Hassan AA. Novel Zeolite 5Å-Co-Fe based catalytic ozonation process for the efficient degradation of oxytetracycline in veterinary pharmaceutical wastewater. Clean Water. 2024. https://doi.org/10.1016/j.clwat.2024.100017.
46. Šuligoj A, Kete M, Černigoj U, Fresno F, Lavrenčič Štangar U. Synergism in TiO2 photocatalytic ozonation for the removal of dichloroacetic acid and thiacloprid. Environ Res. 2021;197:110982. https://doi.org/10.1016/j.envres.2021.110982.
47. Beltrán FJ, Aguinaco A, García-Araya JF. Mechanism and kinetics of sulfamethoxazole photocatalytic ozonation in water. Water Res. 2009;43:1359–69. https://doi.org/10.1016/j.watres.2008.12.015.
48. Nawaz MI, Yi C, Zafar AM, Yi R, Abbas B, Sulemana H, Wu C. Efficient degradation and mineralization of aniline in aqueous solution by new dielectric barrier discharge non-thermal plasma. Environ Res. 2023. https://doi.org/10.1016/j.envres.2023.117015.
49. Nawaz MI, Yi C, Asilevi PJ, Geng T, Aleem M, Zafar AM, Azeem A, Wang H. A study of the performance of dielectric barrier discharge under different conditions for nitrobenzene degradation. Water. 2019;11:842. https://doi.org/10.3390/w11040842.
50. Liao G, Zhu D, Li L, Lan B. Enhanced photocatalytic ozonation of organics by g-C3N4 under visible light irradiation. J Hazard Mater. 2014;280:531–5. https://doi.org/10.1016/j.jhazmat.2014.08.052.
51. Mecha AC, Onyango MS, Ochieng A, Fourie CJS, Momba MNB. Synergistic effect of UV–vis and solar photocatalytic ozonation on the degradation of phenol in municipal wastewater: a comparative study. J Catal. 2016;341:116–25. https://doi.org/10.1016/j.jcat.2016.06.015.
52. Nosaka Y, Nosaka AY. Generation and detection of reactive oxygen species in photocatalysis. Chem Rev. 2017;117:11302–36. https://doi.org/10.1021/acs.chemrev.7b00161.
53. Yu G, Wang Y, Cao H, Zhao H, Xie Y. Reactive oxygen species and catalytic active sites in heterogeneous catalytic ozonation for water purification. Environ Sci Technol. 2020;54:5931–46. https://doi.org/10.1021/acs.est.0c00575.
54. Behnajady MA, Eskandarloo H, Modirshahla N, Shokri M. Influence of the chemical structure of organic pollutants on photocatalytic activity of TiO2 nanoparticles: kinetic analysis and evaluation of electrical energy per order (EEO). Dig J Nanomater Bios. 2011;6:1887–95.
55. Ikhlaq A, Aslam T, Zafar AM, Javed F, Munir HMS. Combined ozonation and adsorption system for the removal of heavy metals from municipal wastewater: effect of COD removal. Desalin Water Treat. 2019. https://doi.org/10.5004/dwt.2019.24164.
56. Shamsi Kasmaei A, Rofouei MK, Olya ME, Ahmed S. Kinetic and thermodynamic studies on the reactivity of hydroxyl radicals in wastewater treatment by advanced oxidation processes. Prog Color, Colorants Coat. 2020;13:1–10. https://doi.org/10.3050/pccc.2020.81596.